3p21.3 Tumor Suppressor Gene *H37/Luca15/RBM5* Inhibits Growth of Human Lung Cancer Cells through Cell Cycle Arrest and Apoptosis

Juliana J. Oh, Ali Razfar, Idolina Delgado, Rebecca A. Reed, Anna Malkina, Baher Boctor, and Dennis J. Slamon

Division of Hematology/Oncology, University of California at Los Angeles School of Medicine, Los Angeles, California

Abstract

Deletion at chromosome 3p21.3 is the earliest and the most frequently observed genetic alteration in lung cancer, suggesting that the region contains tumor suppressor gene(s) (TSG). Identification of those genes may lead to the development both of biomarkers to identify high-risk individuals and novel therapeutics. Previously, we cloned the *H37/Luca15/RBM5* gene from 3p21.3 and showed its TSG characteristics. To investigate the physiologic function of H37 in the lung and its mechanism of tumor suppression, we have stably transfected H37 into A549 non–small cell lung cancer cells. A549/H37 cells show significant growth inhibition compared with the vector controls by *in vitro* and *in vivo* cell proliferation assays. Using this lung cancer cell model, we have found that the molecular mechanism of H37 tumor suppression involves both cell cycle (G_1) arrest and apoptosis. To further define H37's function in cell cycle/apoptotic pathways, we investigated differential expression profiles of various cell cycle and apoptosis regulatory proteins using Western blot analysis. Both cyclin A and phophorylated RB levels were decreased in H37-transfected cells, whereas expression of Bax protein was increased. Mitochondrial regulation of apoptosis further downstream of Bax was investigated, showing change in the mitochondrial membrane potential, cytochrome *c* release into the cytosol, and enhanced caspase-9 and caspase-3 activities. We also report that H37 may mediate apoptosis in a p53-independent manner, and Bax knockdown by small interfering RNA suggests Bax plays a functional role downstream of H37. Lastly, we proposed a tumor suppression model of H37 as a post-transcriptional regulator for cell cycle/apoptotic–related proteins. (Cancer Res 2006; 66(7): 3419-27)

Introduction

The loss of tumor suppressor gene (TSG) function is a critical step in the pathogenesis of human lung cancer. Deletion at chromosome 3p21.3 is the most frequent genetic alteration identified in lung cancer, observed in >90% of small cell lung cancers (SCLC) and in 50% to 80% of non–small cell lung cancers (NSCLC), indicating that the region contains one or more TSGs (1). Furthermore, loss of alleles at a 370-kb region of 3p21.3 is the earliest alteration found in preneoplastic lesions of the lung and sometimes in histologically normal lung epithelium of smokers (2). This timing suggests that 3p21.3 TSGs play a role in preventing lung cancer initiation. Thus, isolation and characterization of the 3p TSGs could be a first step toward developing new targeted treatments and diagnostic tools for lung cancer. Accordingly, the search for TSGs in this region has been the focus of extensive research over the past two decades, and many genes mapping to this region have recently been characterized (3–9). The two most prominent genes, already being evaluated for clinical utility, are *fus-1* (phase I clinical trial; refs. 10, 11) and *RASSF-1A* (epigenetic biomarker; refs. 12, 13).

We previously showed that the *H37* gene (also called *Luca15* or *RBM5*; refs. 14, 15), concurrently cloned by us and others in 1996 and located in the 3p21.3 tumor suppressor region, has the characteristics of a TSG. We found reduced expression (compared with adjacent normal tissue) of the H37 transcript in 9 of 11 (82%) primary NSCLCs (16). By generating a polyclonal H37 antibody and using it for immunohistochemical analysis of primary NSCLC specimens, we further showed that 46 of the 62 (73%) cancers underexpressed H37 protein (16). Moreover, when we introduced H37 cDNA into human breast cancer cells that had 3p21-22 deletions, both anchorage-dependent and anchorage-independent growth was reduced (16). We found that subsequent transfection of H37 cDNA into one of the human lung cancer cell lines with a homozygous deletion in the TSG region (NCI-H740) resulted in a very low yield of H37-expressing clones, suggesting that H37 has antiproliferative properties (16). We also found that H37 suppressed anchorage-dependent and anchorage-independent growth in A9 mouse fibrosarcoma cells and inhibited tumor formation in nude mice (16).

H37's involvement in malignancy has been explored by other investigators as well, with results consistent to our findings. For example, H37 was identified as one of the serum antigens reacting with autologous antibody in renal cancer patients (17). H37/Luca15 is down-regulated in human schwannomas (18) as well as in ras-transformed Rat-1 rat embryonic fibroblastic cells (19). Ectopic expression of the *H37* gene also suppresses growth of HT 1080 human fibrosarcoma cells (19). Several alternatively spliced transcripts from the *H37* locus, and an antisense fragment, seem to function as apoptotic regulators in hematopoetic cells (20–24). In particular, growth inhibition by the full-length H37 correlated with higher apoptotic rates and G_1 cell cycle arrest in CEM-C7 human T cells (24). Most significantly, the *H37/RBM5* gene was included in the 17 common gene signature associated with metastasis (one of the nine genes down-regulated in metastases) identified in multiple solid tumor types (25). Solid tumors carrying this gene expression signature had high rates of metastasis and poor clinical outcome (25). The fact that H37 shows tumor inhibitory properties in multiple different tissues is consistent with the finding that 3p21 is deleted in multiple other tumor types (although not as frequent as in the lung cancer), suggesting that this 3p21.3 TSG may be a general TSG (1).

Note: A. Razfar and I. Delgado contributed equally to this work.

Requests for reprints: Juliana J. Oh, Division of Hematology/Oncology, University of California at Los Angeles School of Medicine, 5-535 MRL, 675 Charles E. Young Drive South, Los Angeles, CA 90095. Phone: 310-206-1408; Fax: 310-825-3761; E-mail: julianaoh@mednet.ucla.edu.

doi:10.1158/0008-5472.CAN-05-1667

Taken together, these data suggest that the *H37* gene plays a significant role in tumor formation. However, tumor suppression by H37 has never been shown, systematically, in the tissue where H37 TSG would presumably be the most important (the lung). Therefore, there remains the need to develop an appropriate lung cancer model to thoroughly test H37 tumor suppression and investigate the physiologic function(s) of H37 and its molecular mechanism of tumor suppression in the most relevant/appropriate tissue type. To this end, we have developed a lung cancer cell line model in which H37 is ectopically expressed. By using this cell system, we have confirmed tumor suppressive activity of H37 in the lung and begun to characterize the molecular mechanism/biochemical pathways for H37's tumor suppression.

Materials and Methods

Cell culture. A549 cells were purchased from the American Tissue Type Collection (Manassas, VA). Cells were grown in RPMI 1640 supplemented with 10% fetal bovine serum, 2 mmol/L glutamine, and 1% penicillin G/streptomycin/fungizone solution.

Plasmid transfection and generation of stable H37 transfectants. The full-length H37 cDNA was subcloned in the pBK-CMV eukaryotic expression vector. The plasmid was transfected into cells by LipofectAMINE (Invitrogen, Carlsbad, CA) according to the manufacturer's protocol. After selection in G418 (700 μg/mL) for 2 weeks, cells were plated into 10-cm dishes at limiting cell dilutions. Single cells that grew into individual colonies were removed from the dish by cell scraping and transferred into a six-well plate. Each cell line was then expanded and tested for H37 expression. The transfected cells were strictly maintained in the same concentrations of G418 to avoid reversion of the cells.

Cell counts and soft agar assay. Cells were plated in triplicate in six-well plates (5,000 per well). After plating (day 0), seeding density was measured at day 1, and cells were counted at days 3, 5, and 7 by Coulter cell counter. For soft agar assay, cells were plated in 0.5% (bottom) and 0.3% (top) soft agar layers, in triplicate, in 35-mm dishes (20,000 per dish) and were incubated for up to 2 weeks before counting and photography. Colonies with >20 cells were counted.

Cell cycle analysis. Cells (1×10^6) were harvested and washed in cold PBS followed by fixation in 70% alcohol for 30 minutes on ice. After washing in cold PBS three times, cells were resuspended in 0.8 mL of PBS solution with 40 μg of propidium iodide and 0.1 μg of RNase A for 30 minutes at 37°C. Samples were analyzed for DNA content by FACSCalibur (Becton Dickinson, San Jose, CA) using blue 488-nm laser for excitation and fl2 detector 585 ± 21 nm for emission.

Hoechst staining for apoptotic cell nuclei. Cells grown in four-well chamber slides (8,000 per chamber) were fixed in Carnoy's Fixative (one part glacial acetic acid to three parts absolute methanol; MP Biochemicals, Irvine, CA) and subsequently stained with Hoechst 33258 (0.05 μg/mL) in HBSS (MP Biochemicals). The cells were observed under a fluorescence microscope, and blue cells with apoptotic nuclear characteristics, such as nuclear condensation and fragmentation, were scored as apoptotic. Results are expressed as the percentage of the number of apoptotic cells compared with the total number of cells in 10 random 0.159-mm^2 fields.

Terminal deoxynucleotidyltransferase–mediated nick end labeling staining. The assay was done using the *In situ* Cell Death Detection kit, Fluorescein (Roche Applied Science, Indianapolis, IN), according to the manufacturer's instructions for adherent cell preparations. A terminal deoxynucleotidyltransferase–mediated nick end labeling (TUNEL) reaction mixture without terminal transferase served as a negative control. For a positive control, permeabilized cells were incubated with DNase I for 10 minutes at 15°C to 25°C to induce DNA strand breaks before labeling procedures. Cells plated onto microscope slides were air-dried and fixed with 4% paraformaldehyde (pH 7.4) for 1 hour, then incubated in 0.1% Triton X-100 with 0.1% sodium citrate on ice for 2 minutes. Fifty microliters of the TUNEL reaction mixture containing fluorescein-dUTP and terminal deoxynucleotidyl transferase were added to the cells with subsequent incubation in a humidified chamber for 60 minutes at 37°C in the dark. Apoptotic cells exhibiting a strong nuclear green fluorescence were detected using a standard fluorescein filter (520 nm). To quantify the apoptotic events, the number of cells undergoing apoptosis was counted in ten 0.159-mm^2 fields and expressed as a percentage of the total number of tumor cells in the same field.

Western blot analysis. Western blot analysis was done according to the standard protocol (26). Antibodies for the cell cycle–related proteins were purchased from Santa Cruz Biotechnology (Santa Cruz, CA), and all the antibodies for apoptotic pathways were purchased from BD Biosciences (San Jose, CA).

Bax knockdown by small interfering RNA. The SMARTpool small interfering RNA (siRNA; Dharmacon, Lafayette, CO) for Bax was used, which contains a mixture of four siRNA duplexes selected by the SMARTselection algorithm by the manufacturer. The siRNA transfection was done using the DharmaFECT1 transfection reagent (Dharmacon) according to the manufacturer's instructions. Briefly, A549 cells were seeded in 24-well plates (1.25×10^4 in 0.5 mL per well) in antibiotic-free growth media 1 day before the transfection. For transfection, the growth media was replaced with the 500 μL of the transfection mixture (per well) containing 50 pmol siRNA and 2 μL DharmaFECT1 in the Opti-MEM I–reduced serum medium (Invitrogen). The transfection medium was replaced with the complete growth medium 24 hours after the transfection. The cells were harvested 96 hours after the transfection for the Bax expression analysis by Western blot and cell counts and TUNEL assays. Appropriate controls (all from Dharmacon) were used as follows: siGlow and siTox (positive transfection controls), siGAPDH (positive knockdown control), and siNon-Targeting Pool (negative control).

Mitochondrial membrane potential breakdown assay. Cells were seeded in four-well chamber slides 24 hours before staining. Cells were stained with the JC-1 reagent (Stratagene, La Jolla, CA) and incubated in the tissue culture incubator for 15 minutes according to the manufacturer's protocol. JC-1 aggregates in the mitochondria (only in live cells) were detected as the red color by a fluorescence microscope at excitation/emission = 540/570 nm; JC-1 monomers in the cytosol (in both live and apoptotic cells) were detected as green at excitation/emission = 490/520 nm.

Cytochrome *c* release assay. Cell fractionation was done by using the cytochrome *c* release apoptosis assay kit (Calbiochem, San Diego, CA) according to the manufacturer's protocol. Briefly, the cell pellet (5×10^7 cells) was resuspended in 1 mL cytosol extraction buffer mix containing DTT and protease inhibitors, incubated on ice for 10 minutes, and disrupted with 30 to 50 passes of a Dounce homogenizer. The homogenate was centrifuged at $700 \times g$ to separate the pellet containing the nuclei, unbroken cells, and large membrane fragments from the supernatant containing cytosolic fraction. The pellet was resuspended in 0.1 mL mitochondrial extraction buffer mix to obtain mitochondrial fraction; 10 μg of each cytosolic and mitochondrial fraction was subjected to 12% SDS-PAGE electrophoresis and Western blot analysis with the monoclonal cytochrome *c* antibody.

Caspase-9 and caspase-3 activity assays. Caspase-9 activity was analyzed using a fluorometric assay kit (R&D Systems, Minneapolis, MN) according to the manufacturer's instructions. Briefly, the cell pellet (1×10^6 cells) was lysed in the lysis buffer on ice. After protein standard assay, 50 μL of cell lysate containing 125 μg of protein and the reaction buffer was pipetted into a 385-well plate. Subsequently, 5 μL of caspase-9 fluorogenic substrate [LEHD peptide conjugated to 7-amino-4-trifluoromethyl coumarin (AFC)] was added to each reaction well. After 1 hour of incubation at 37°C, the plate was read in a fluorescence microplate reader (Flexstation II, Molecular Devices, Sunnyvale, CA) at 400 and 505 nm excitation and emission wavelengths, respectively.

Caspase-3 activity was analyzed using a fluorometric immunosorbent enzyme assay kit (Roche Applied Science) according to the manufacturer's instructions. Briefly, caspase-3 from cellular lysates (2×10^6 cells) was captured by a monoclonal anti-caspase-3 antibody precoated to the microtiter plate. Following the washing step, added substrate (Ac-DEVD-AFC) was cleaved proportionally to the amount of activated caspase-3.

Generated free fluorescent AFC was determined fluorometrically at 505 nm. Results are reported as formed AFC (μmol/L) as determined against a standard curve.

Results

Screening of multiple adherent lung cancer cells for the H37 protein expression and the *H37* gene transfection. Prior experiments designed to ectopically express H37 in lung cancer cells, which were deleted at 3p21.3, were limited due to the cell line availability (16). The NCI-H740 cells would have been an ideal model system to test because both copies of 3p21.3 are deleted. However, they grow in suspension and are difficult to maintain in culture. Thus, we were only able to show H37's growth inhibition to a limited extent (16) because we could not grow the cells on soft agar for anchorage-independent growth assay nor generate stable transfectant cell clones to further characterize biochemical pathways of H37 tumor suppression. As an alternative strategy, we screened multiple adherent lung cancer cell lines to compare H37 protein expression levels. We found that among seven commonly used adherent lung cancer cell lines, A549 cells have the lowest H37 protein expression by Western blot analysis (Fig. 1*A*). These cells were used as parental cells for H37 transfection using pBK-CMV plasmid expression vector. Both transiently (3 days after transfection) and throughout the 2-week selection in neomycin, the H37 transfectants showed consistent growth retardation compared with the vector controls (Fig. 1*B*). The A549/H37 cells grew to only 20% of the control cells at the end of the 2-week selection period (data not shown). Morphologically, examination of the control cells revealed organized, tightly packed, uniform-shaped cancer cell colonies with a "cobblestone" appearance, whereas the H37 cells displayed an irregular, disorganized array of colonies consisting of flattened giant cells with cytoplasmic extensions (Fig. 1*B*). This disordered cell feature has been reported to be related to TSG transfections with other genes, including *p53* (27).

Generation of stable clones and cell proliferation assays. To generate stable transfectants with defined levels of H37 expression, numerous single transfected cells were expanded to cell clones. As expected, these cells were difficult to propagate due to the growth inhibition induced by H37. A total of 28 H37 clones and 12 control clones were generated, and H37 expression levels in each clone were analyzed by Western blot analysis. H37 expression levels from two representative H37 clones (hereafter called H1 and H2) and two control clones (hereafter called C1 and C2) are shown in Fig. 2*A*. To measure proliferation rates, growth curves were generated for each clone over a 1-week period. By day 7, growth of H1 and H2 cells was reduced by 78% and 72%, respectively, compared with the average control level. In addition, significantly reduced numbers (as well as size) of the soft agar colonies resulted from H37 transfection in an anchorage-independent growth assay (Fig. 2*C*). The numbers of H1 and H2 colonies were reduced by 69% and 76%, respectively, compared with the average control levels (Fig. 2*C*). Subsequently, growth inhibition of the H37-overexpressing A549 cells were further evaluated by s.c. injection into nude mice. In contrast to the control cells that formed relatively large tumors within a short period of time, animals injected with H37.1 and H37.2 cells exhibited almost complete inhibition of tumor formation (Fig. 2*D*).

Analysis of cell cycle alterations induced by H37. We next explored the mechanisms underlying growth inhibition by H37. The lack of growth in H37 transfectants may result from cell cycle effects, cell death, or a combination of the two processes. The cell cycle distribution of cells transfected with control vectors or H37 was determined by fluorescence-activated cell sorting analysis of propidium iodide–stained cells, a measure of DNA content. As shown in Fig. 3*A*, H37 clones showed a higher proportion of cells in G_0-G_1 phase (69.44% and 61.71% for H1 and H2, respectively), compared with control cells (50.73% and 49.67% for C1 and C2, respectively), and a concomitant decrease in the proportion of cells in S phase (22.32% and 25.28% for H1 and H2, respectively) relative to that observed in controls (39.11% and 37.51% for C1 and C2, respectively).

Analysis of apoptosis induced by H37. To determine the contribution of cell death to H37-induced reductions in cell growth, we employed two different methods to detect apoptotic cells: Hoechst staining and TUNEL labeling. Hoechst staining, by fluorescence detection, enables more direct visualization of apoptotic cells, which undergo compaction and fragmentation of the nuclear chromatin, shrinkage of the cytoplasm, and loss of

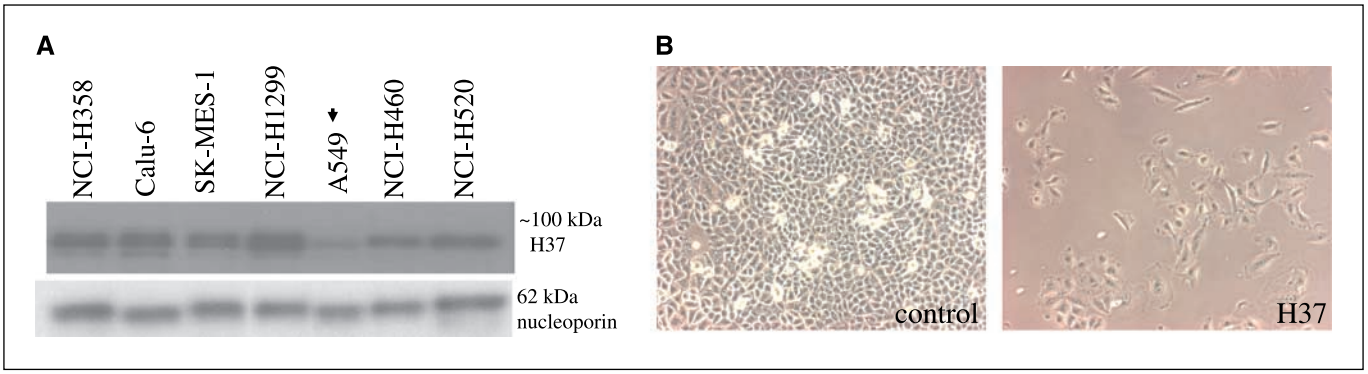

Figure 1. *A,* screening of multiple adherent lung cancer cell lines for H37 protein expression. Seven lung cancer cell lines were compared for H37 protein expression levels by Western blot analysis. Experiments were done with either whole cell or purified nuclear extracts (i.e., H37 is a nuclear protein; ref. 16), and the consistent results were obtained from both types (shown here is a data obtained from nuclear extract). The polyclonal recombinant H37 antibody used here is previously described (16). A549 cells were chosen for the H37 plasmid transfection. Nucleoporin expression was used as a protein loading control. *B,* H37 transfection into A549 cells and comparison of colony growth and morphology between H37 transfectants and vector control cells. The H37 containing plasmid (pBK-CMV/H37) was transfected into A549 cells, and growth rate and morphology were compared between the H37 and the vector control cells. Photographs taken at the end of the 2-week selection in G418 (700 μg/mL) and immediately before generation of single-cell expanded clonal populations. Whereas the control cells exhibit characteristic features of cancer cell colonies, including a tightly packed, uniform-shaped ''cobblestone'' appearance, the H37 cells show changes observed with TSGs, such as disorganized colonies of flattened giant cells with cytoplasmic extensions.

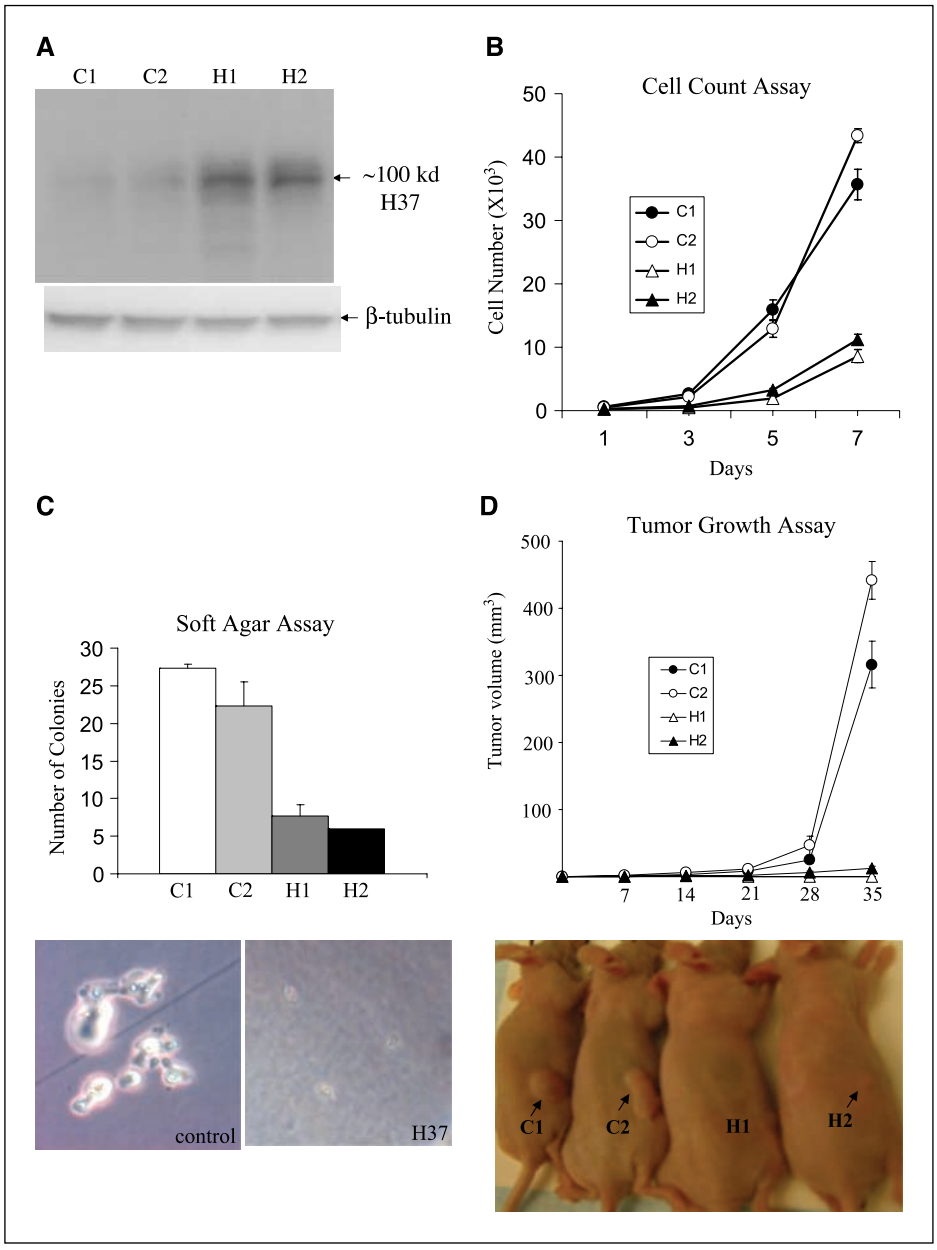

Figure 2. Generation of stable H37 clones and cell proliferation assays. *A,* comparison of H37 expression levels in single-cell expanded clones. Western blot showing H37 protein expression achieved in the two representative control clones (C1 and C2) and the two representative H37 clones (H1 and H2). β-Tubulin expression was used for a protein loading control. *B,* growth curve of H37-transfected A549 cells. The cells were plated in triplicate in six-well plates (5,000 in 2 ml of medium per well). After plating (day 0), seeding density was measured at day 1, and cells were counted at days 3, 5, and 7 by Coulter cell counter. *C,* soft agar colony assay. Cells (20,000 per 35-mm dish) were cultured in soft agar medium. Two weeks later, colonies of >20 cells were counted. *Photos,* a representative colony each from the vector control and the H37 transfectants. *D,* tumor formation in nude mice. Cells (1×10^7) of the A549 transfectants were injected into mid-back region of mice (9 mice per group). Tumors were measured in three dimensions on the indicated days. Appearances of representative tumors from each cell type; taken at day 35 after inoculation.

membrane asymmetry. As shown in Fig. 3*B*, condensed and fragmented nuclei were more frequently observed in H37-transfected cells and were only rarely seen in the control cells (~ 3.5-fold increase in the H37 cells compared with the control). These findings were confirmed by TUNEL assay, in which labeled uridine bases are attached to the DNA nicks characteristic of apoptotic cells showing green fluorescence. As shown in Fig. 3*C*, approximately three times more of the H37 cells were apoptotic compared with the control cells. In addition, most of the cells counted apoptotic showed stronger intensity of green in the H37 cells.

Analysis of cell cycle– and apoptosis-regulated proteins in association with H37 overexpression. To investigate potential molecular mechanisms for H37-induced cell cycle alterations and apoptosis, we examined the effects of H37 on cell cycle and apoptosis regulatory proteins. Whole-cell protein extracts prepared from either the H37 and/or control A549 cells were analyzed for protein levels by Western blotting. Although a spectrum of cell cycle regulatory proteins was tested, including p53, pRB, cyclins A, B, C, D1, D2, D3, and E, p21, p27, cyclin-dependent kinase 2 (cdk2), cdk4, and cdk7/CAK, we detected noticeable changes in only two proteins, cyclin A and hyperphosphorylated RB, both of which were down-regulated in H37 cells (Fig. 3*D*). There were no marked changes in expression level in any of the other proteins tested (data not shown). Both cyclin A and hyperphosphorylated RB function in progressing cells from G_1 to S phase, and a decrease expression of these proteins is consistent with the G_1 arrest induced by H37. Similarly, of a large number of apoptosis regulatory proteins tested (p53, Bad, Bax, Bcl-2, Bcl-x, caspase-2, caspase-3, caspase-7, DFF45, FADD, Fas, PARP, Apaf-1, and CAS), we observed a significant alteration in only one protein, the proapoptotic protein Bax. Its expression was increased significantly in the H37 cells (Fig. 3*D*). Bax, downstream of p53, promotes apoptosis by triggering caspases cascades in apoptotic pathways, and its increased expression in H37 cells is consistent with increased apoptotic rates in H37 cells.

H37 transfection into the p53-null lung cancer cells. Our observation that H37-induced tumor suppression is not associated with a change in p53 protein expression in A549 cells prompted us to test a hypothesis that H37 may suppress tumor growth independently of p53. To this end, we transfected H37 into the H1299 human NSCLCs (p53 deleted) in parallel with A549 and H460 cells (both p53 wild type). Despite lack of p53, H1299 cells, upon H37 transfection, still manifested reduced cell proliferation and increased apoptosis

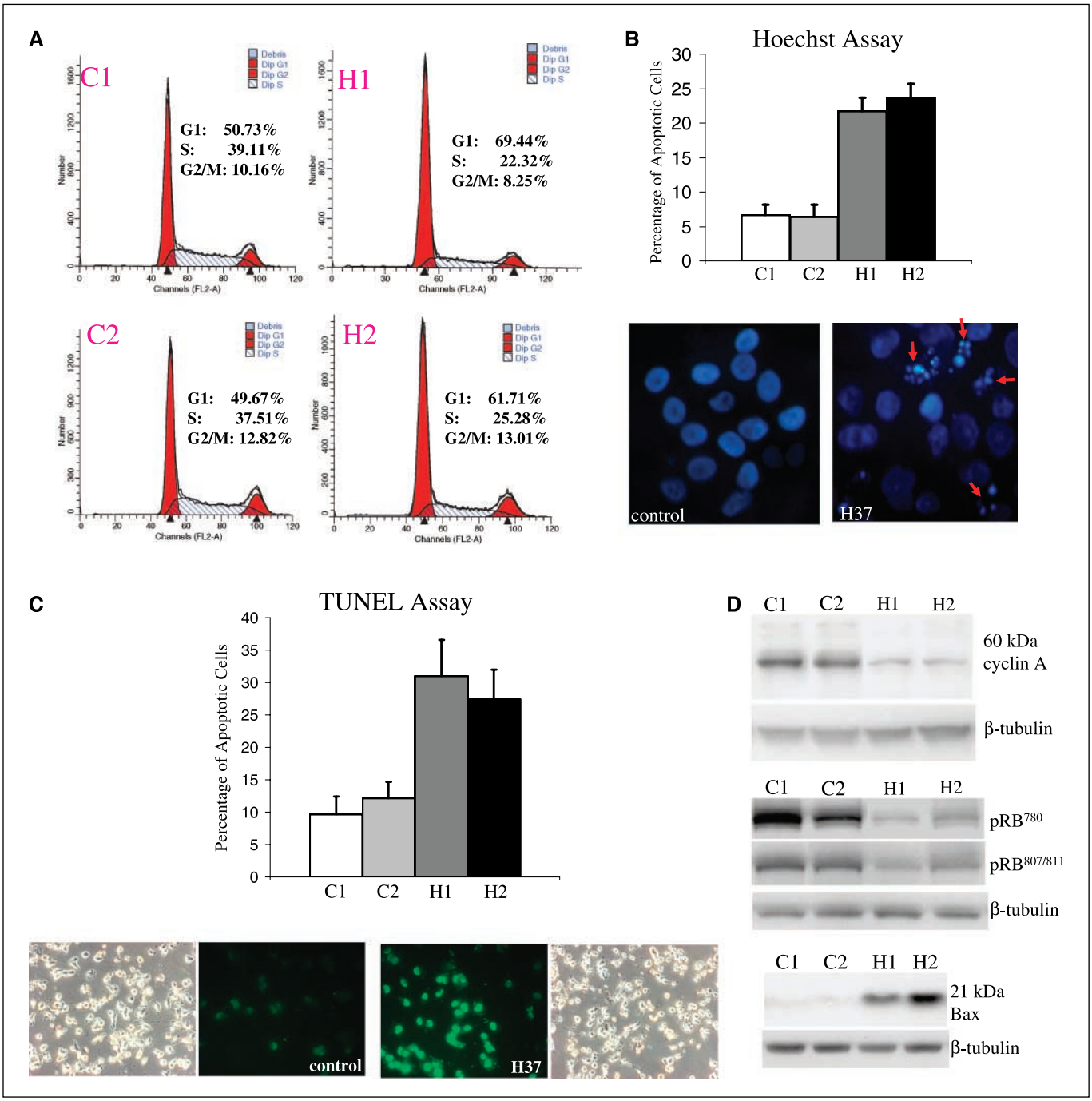

Figure 3. Analysis of cell cycle– and apoptosis-regulated proteins associated with H37 overexpression. *A,* cell cycle analysis of H37 and control A549 cells. Propidium iodide staining followed by flow cytometry was used to analyze cell cycle distribution. H37 transfection resulted in an increased proportion of cells in the G_1 phase and a decreased proportion of cells in the S phase. *B,* analysis of H37- induced apoptosis by Hoecht staining. Control and H37-transfected A549 cells were stained with Hoechst 33258 (0.055 μg/mL) and visualized under fluorescence microscopy. Representative areas each from the control and H37 cells illustrate DNA fragmentation (*arrows*) as a sign of apoptosis, which is more frequently detected in H37 cells. *C,* H37-induced apoptosis shown by TUNEL staining. Control and H37-transfected A549 cells were treated with terminal deoxynucleotidyl transferase to incorporate fluorescein-dUTP to nicked DNA of apoptotic cells. Apoptotic cells exhibiting a strong nuclear green fluorescence were detected by fluorescence microscopy and compared between the two cell types. Adjacent light microscopic photos show a representative area from each cell type showing equal cell density and fixation. *D,* differential expression of the cell cycle and apoptosis regulatory proteins associated with H37 overexpression. Western blot analysis was done to compare expression levels of various cell cycle– and/or apoptosis-related proteins between the control and H37-transfected A549 cells. Among them, cyclin A and phospho-RB (cell cycle related) expressions were found to be decreased and Bax (apoptosis related) increased in the H37 cells compared with the control. β-Tubulin was used as a protein loading control.

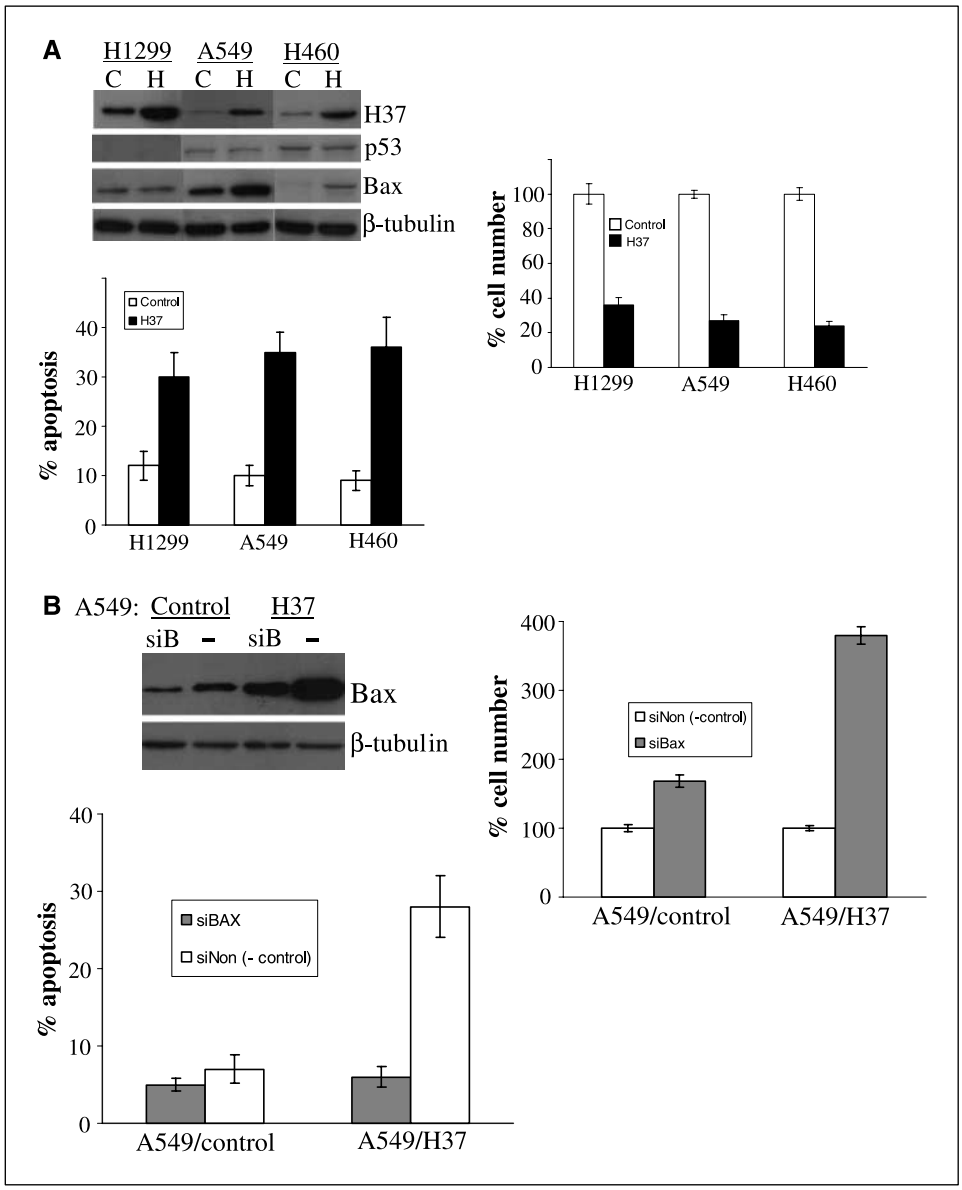

Figure 4. Analysis of functional involvement of p53 and Bax in H37-mediated apoptosis. *A,* H37 transfection into the p53- null H1299 lung cancer cells. The H37 and the control plasmids were transfected into H1299, A549, and H460 lung cancer cells as described in Materials and Methods. At the end of the 2-week selection in G418 (800, 700, and 500 μg/mL concentrations, respectively), the transfected cells were harvested for cell counts, TUNEL apoptotic assay, and Western blot analysis (for H37, p53, and Bax protein expression, the same membrane was restriped and reprobed; β-tubulin as a protein loading control). *B,* Bax knockdown by siRNA in A549/H37 versus control cells. The Bax protein expression was analyzed 96 hours after siRNA transfection, at which point cells were also compared for proliferation (by cell counts, numbers adjusted to % negative siRNA control transfectant for the respective cell types) and for apoptosis (by TUNEL assay). The negative control used was the pool of four nontargeting siRNAs (*siNon*), each bioinformatically designed to minimize the potential for targeting any known human or mouse genes. *Left,* Bax siRNA (*siB*) and negative control (–) transfections.

(Fig. 4*A*). These changes were comparable with the levels seen in the A549/H37 and H460/H37 transfectants, although we could not detect any noticeable change in Bax protein expression in the H1299/H37 cells in contrast to the A549/H37 and the H460/H37 cells (Fig. 4*A*). Bax may not be active/functional in H1299 cells due to lack of its immediate upstream activator, p53, and/or other potential biochemical alterations associated with p53's absence; therefore, H37 may initiate mitochondrial apoptotic pathway through molecules further downstream of Bax in this cell line. The possibility still exists that H37- induced change in p53 protein expression level may be too subtle to be detected by Western blot, or p53 is activated by post-translational modifications and/or by any other alternative mechanisms in the p53 wild-type A549/H37 and H460/H37 cells. Nonetheless, our preliminary data showing inhibition of growth by H37 in the p53- null lung cancer cells may suggest existence of a novel, H37-mediated apoptotic pathways operating independent of the p53 regulations. It is intriguing to note that the p53-null H1299 has the highest H37 expression level (Fig. 1*A*), and investigation of multiple other p53-null lung cancer cells is warranted.

Analysis of Bax's biological involvement in H37-mediated apoptosis using Bax siRNA. To further confirm that Bax plays a direct functional role downstream of the H37-induced apoptotic pathway, we employed siRNA knockdown to reverse Bax expression comparable with the level seen in the A549/control cells (Fig. 4*B*). Bax knockdown in A549/H37 cells showed 280% increase in cell proliferation and 79% decrease in apoptotic rate compared with the negative control siRNA transfection (Fig. 4*B*). These changes are in contrast to the only 68% increase and 29% decrease, respectively, observed in the A549/control cells (Fig. 4*B*). The reverted growth properties in the H37 cells upon knockdown of Bax expression (which was initially induced by H37) suggests Bax functions biologically in the downstream of H37 in A549 cells.

H37-induced mitochondrial apoptotic pathways. To further characterize the molecular mechanisms of the H37/Bax–mediated

apoptotic pathways, we investigated the influence of mitochondrial apoptosis signaling. Fluorescence microscopy following JC-1 staining revealed breakdown of mitochondrial membrane potential by H37. As shown in Fig. 5*A*, decrease in mitochondrial red staining in the H37 cells (due to loss of JC-1 aggregates in the mitochondria) indicated reduced mitochondrial membrane potential, and the number of the cells with intact mitochondrial membrane potential was shown to be decreased in H1 and H2 by 47% and 43%, respectively, over the average control level. Thus, the contents of the inter membrane space, including cytochrome *c*, were released into the cytosol in the H37 cells (Fig. 5*B*). Subsequently, cytochrome *c* accumulated in the cytosol-triggered caspase-9 activity, 96% and 83% increase in H1 and H2, respectively, over the average control level (Fig. 5*C*). Caspase-9, in turn, activated its downstream caspase-3, 78.8% and 88.2% increase in H1 and H2, respectively, over the average control level (Fig. 5*D*). The activated caspase-3 is responsible for the cytologic changes characteristic of apoptosis, including DNA fragmentation. The current data suggest that although H37's involvement in the death receptor–mediated apoptotic pathway remains to be in depth investigated, H37-mediated growth suppression, at least in part, employs regulation of mitochondrial apoptotic pathways.

Discussion

The earliest and most common genetic change observed in lungs of smokers maps to the short arm of chromosome 3, specifically, 3p21.3 (1). This is the region where deletions are observed most frequently in lung cancer, and occasionally, the whole band is homozygously deleted. These observations suggest that TSGs reside at 3p21.3. The fact that specific alterations at this location can be detected in preneoplastic or preinvasive lesions also suggests that one or more 3p TSGs may function as "gatekeepers" for initiation of carcinogenesis and hence hold particular promise as biomarkers as well as potential therapeutic targets. Such biomarkers could be used to (*a*) identify individuals at high risk for lung cancer, (*b*) diagnose early lung cancer, and (*c*) assess the efficacy of lung cancer therapies and chemopreventive agents. In addition, 3p-linked biomarkers could have prognostic value.

H37/Luca15/RBM5 is among the 35 genes located within the 370-kb minimal area of deletions at 3p21.3 (14). The current report represents the first characterization of H37 tumor suppressive activity in lung cancer cells. The data showed that H37 inhibition of human lung cancer cell growth involves both interference with cell cycle progression and induction of apoptosis. Among the various cell cycle–regulated proteins tested, we have identified decreased cyclin

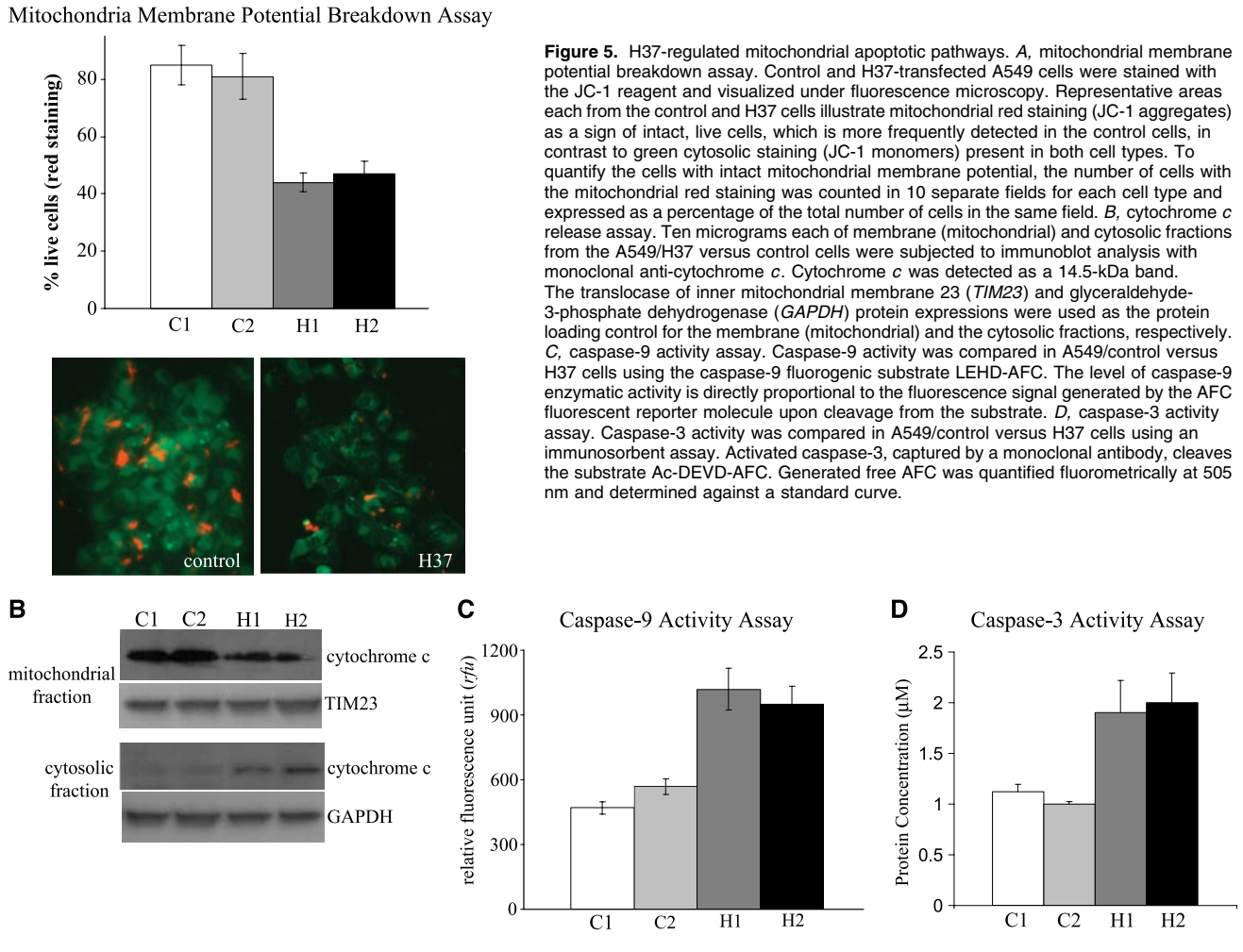

Figure 5. H37-regulated mitochondrial apoptotic pathways. *A,* mitochondrial membrane potential breakdown assay. Control and H37-transfected A549 cells were stained with the JC-1 reagent and visualized under fluorescence microscopy. Representative areas each from the control and H37 cells illustrate mitochondrial red staining (JC-1 aggregates) as a sign of intact, live cells, which is more frequently detected in the control cells, in contrast to green cytosolic staining (JC-1 monomers) present in both cell types. To quantify the cells with intact mitochondrial membrane potential, the number of cells with the mitochondrial red staining was counted in 10 separate fields for each cell type and expressed as a percentage of the total number of cells in the same field. *B,* cytochrome *c* release assay. Ten micrograms each of membrane (mitochondrial) and cytosolic fractions from the A549/H37 versus control cells were subjected to immunoblot analysis with monoclonal anti-cytochrome *c*. Cytochrome *c* was detected as a 14.5-kDa band. The translocase of inner mitochondrial membrane 23 (*TIM23*) and glyceraldehyde-3-phosphate dehydrogenase (*GAPDH*) protein expressions were used as the protein loading control for the membrane (mitochondrial) and the cytosolic fractions, respectively. *C,* caspase-9 activity assay. Caspase-9 activity was compared in A549/control versus H37 cells using the caspase-9 fluorogenic substrate LEHD-AFC. The level of caspase-9 enzymatic activity is directly proportional to the fluorescence signal generated by the AFC fluorescent reporter molecule upon cleavage from the substrate. *D,* caspase-3 activity assay. Caspase-3 activity was compared in A549/control versus H37 cells using an immunosorbent assay. Activated caspase-3, captured by a monoclonal antibody, cleaves the substrate Ac-DEVD-AFC. Generated free AFC was quantified fluorometrically at 505 nm and determined against a standard curve.

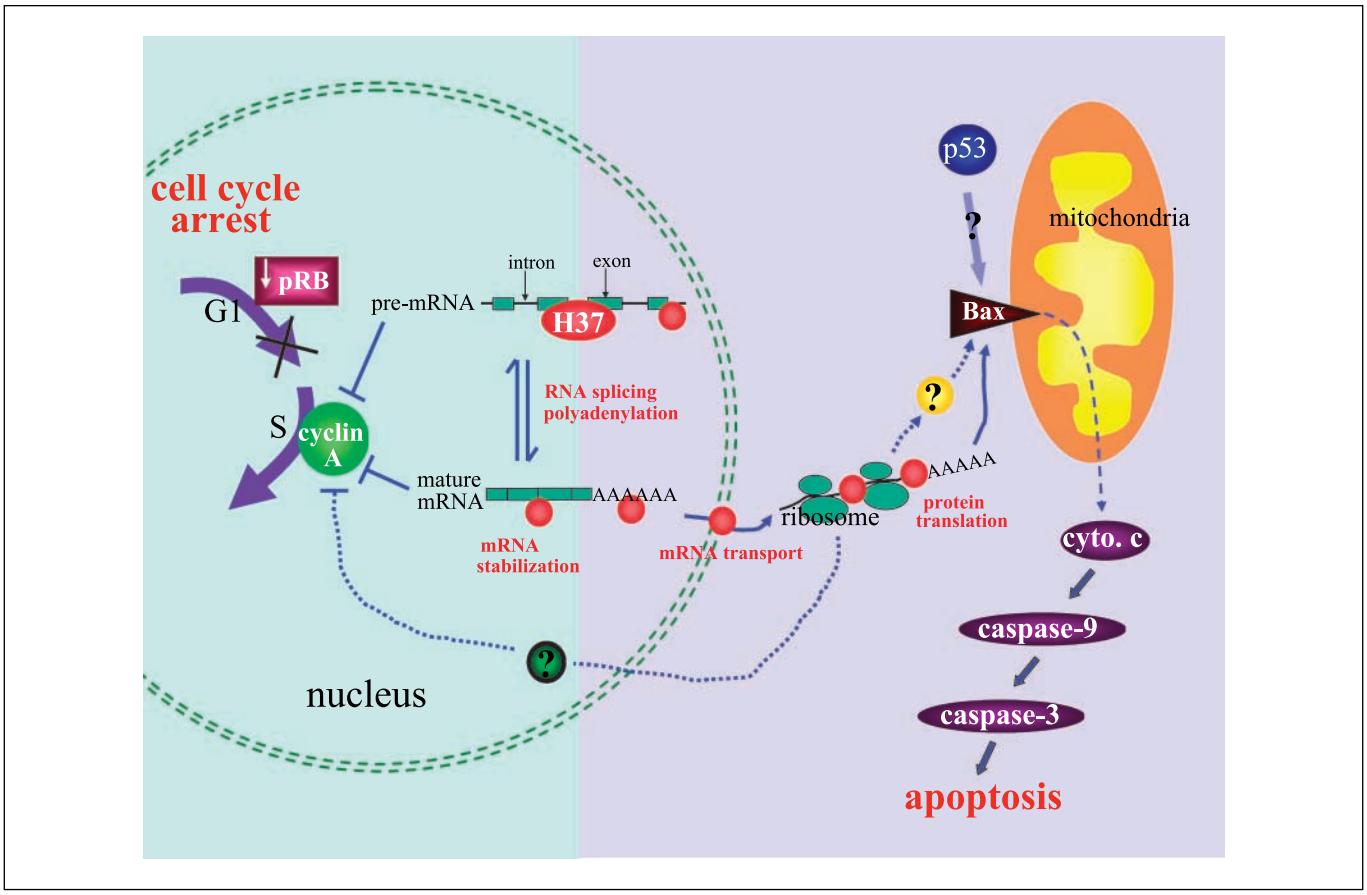

Figure 6. A proposed model summarizing the role of H37 in tumor suppression. The proposed model suggests that the H37 protein (illustrated as the red circles) with RNA binding capacity may participate in one or more different processes in post-transcriptional regulation pathways (i.e., RNA splicing, polyadenylation, message stability, mRNA transport, protein translation, etc.). H37, depending on either the "activating" or "inhibitory" binding (to RNA transcripts), may facilitate or impede generation of proteins (i.e., Bax or cyclin A, respectively) involved in tumor suppression or any other unknown proteins (illustrated as a question mark within the circles) upstream of either apoptotic (Bax) or cell cycle (cyclin A) pathways.

A and phosphorylated RB to be associated with H37 overexpression. In G_1 phase, the cyclin D–dependent kinases initiate Rb phosphorylation, activating cyclin E for S-phase entry (28). Cyclin E/cdk2 then completes RB phosphorylation at the G_1-S transition, after which cyclin E is degraded and replaced by cyclin A during the S phase (28). The data showing H37-induced decreases in cyclin A and phospho-RB protein expression are consistent with the decreased proportion of S-phase cells and increased proportion of G_1 phase cells observed in these studies. The precise mechanism by which these events are achieved remains to be clarified, and studies are in progress to elucidate the potential signaling pathway(s) involved in H37 growth inhibition by G_1 phase cell cycle arrest.

Apoptosis is a complex, multistage process involving many genes. Among the wide spectrum of apoptosis regulatory proteins tested in our studies, the proapoptotic protein Bax was found to be overexpressed in H37-overexpressing lung cancer cells, with concomitant triggering of the mitochondrial apoptotic pathways, including caspase-9 and caspase-3 activations. A major regulation of the apoptotic death signal resides with the *bcl-2/bax* genes, the former an apoptosis-suppressing and the latter an apoptosis-promoting protein (29). Bax and Bcl-2 can form heterodimers, and overexpression of one antagonizes the other's effect; p53 functions, in part, by regulating the ratio of Bax/Bcl-2. In our studies, bcl-2 expression was not changed in the H37 cells. Thus, H37 expression may result in increased bax protein expression, leading to an increased apoptotic rate.

In an attempt to understand further the cellular/molecular functional mechanism of the H37-mediated tumor suppression, we have recently done computational algorithms to search for the transcription factor binding sites commonly present in the *H37* gene promoter across species. Among those predicted to be true transcription factor binding sites was for the ZNF143/STAF protein, a transcription factor for eight different vertebrate small nRNA genes that function in RNA processing, such as splicing and polyadenylation (30, 31). This finding, although it needs to be validated by actual experiments, such as a gel-shift assay, is in a good correlation with the previous observations that the H37 protein contains RNA-binding motifs (i.e., RBM5 is another name for H37/Luca15; refs. 15, 32), and H37 shows *in vitro* RNA-binding activity (33). Taken together, our current hypothesis is that H37 may function in some aspects of post-transcriptional regulations of certain important proteins involved in cell cycle and/or apoptosis (i.e., Bax, cyclin A, RB, etc.). Based on this idea and in summary of our current findings, here, we propose a putative model for the molecular/cellular mechanism of the H37-mediated tumor suppression (Fig. 6). In this model, the RNA-binding protein H37 may directly interact with mRNA transcripts of certain important regulatory proteins involved in tumor formation, either stabilizing tumor-suppressing genes

(i.e., *Bax*) and/or destabilizing tumor-promoting genes (i.e., *cyclin A*; Fig. 6). The RNA-binding proteins control mRNA stability and translation of the specific target mRNAs through a complex network of RNA/protein interactions. HuR, mdm-2, and VHL are only the few examples of an ever-increasing number of RNA-binding proteins carrying out important functions in cancer (34). Identification of the specific mRNA targets of H37 and/or its RNA-protein complex warrants future investigations.

The A549/H37 versus control cell pair system may be further used to examine H37's role in various physiologic pathways (e.g., transformation prevention, growth signal transduction, differentiation, genomic stability, and DNA damage response). This system may also be used for identifying downstream target molecules involved in the H37 growth suppression pathway. The genes differentially expressed in association with H37 growth inhibition are being studied by microarray analyses comparing the two cell populations differing only in H37 expression level, and we hope that these data will yield better insights into the cellular function of H37. The isogenic cell paired system may also be used to identify H37 protein partners or to validate the found partners by the yeast two-hybrid screening, which is currently under way. However, the most rigorous test of validating H37 as a bona fide tumor suppressor could come from generation of H37 knockout mice, and these studies are currently in progress.

In sum, the current studies provide a foundation to further explore the role of H37 in lung cancer pathogenesis and suggest a strategy for the development of rationally designed therapeutics using H37 as a target.

Acknowledgments

Received 5/17/2005; revised 1/23/2006; accepted 1/31/2006.

Grant support: Developmental Research Program Award from the University of California at Los Angeles Lung Cancer Specialized Programs of Research Excellence grant P50 CA90388 (J.J. Oh), American Lung Association of California Research Grant (J.J. Oh), and the Wolfen Family Lung Cancer Clinical/Translational Research Program at University of California at Los Angeles Jonsson Comprehensive Cancer Center.

The costs of publication of this article were defrayed in part by the payment of page charges. This article must therefore be hereby marked *advertisement* in accordance with 18 U.S.C. Section 1734 solely to indicate this fact.

We thank Dr. David Reese for helpful discussion of this manuscript and Dr. Robert Damoiseaux at University of California at Los Angeles Molecular Shared Screening Resources for his help with caspase-9 activity assay.

References

1. Lerman MI, Minna JD. The 630-kb lung cancer homozygous deletion region on human chromosome 3p21.3: identification and evaluation of the resident candidate tumor suppressor genes. The International Lung Cancer Chromosome 3p21.3 Tumor Suppressor Gene Consortium. Cancer Res 2000;60:6116–33.
2. Wistuba II, Lam S, Behrens C, et al. Molecular damage in the bronchial epithelium of current and former smokers. J Natl Cancer Inst 1997;89:1366–73.
3. Carboni GL, Gao B, Nishizaki M, et al. CACNA2D2-mediated apoptosis in NSCLC cells is associated with alterations of the intracellular calcium signaling and disruption of mitochondria membrane integrity. Oncogene 2003;22:615–26.
4. Qiu GH, Tan LK, Loh KS, et al. The candidate tumor suppressor gene BLU, located at the commonly deleted region 3p21.3, is an E2F-regulated, stress-responsive gene and inactivated by both epigenetic and genetic mechanisms in nasopharyngeal carcinoma. Oncogene 2004;23:4793–806.
5. Dammann R, Li C, Yoon JH, Chin PL, Bates S, Pfeifer GP. Epigenetic inactivation of a RAS association domain family protein from the lung tumour suppressor locus 3p21.3. Nat Genet 2000;25:315–9.
6. Ji L, Nishizaki M, Gao B, et al. Expression of several genes in the human chromosome 3p21.3 homozygous deletion region by an adenovirus vector results in tumor suppressor activities *in vitro* and *in vivo*. Cancer Res 2002;62:2715–20.
7. Tse C, Xiang RH, Bracht T, Naylor SL. Human Semaphorin 3B (SEMA3B) located at chromosome 3p21.3 suppresses tumor formation in an adenocarcinoma cell line. Cancer Res 2002;62:542–6.
8. Kashuba VI, Li J, Wang F, et al. RBSP3 (HYA22) is a tumor suppressor gene implicated in major epithelial malignancies. Proc Natl Acad Sci U S A 2004;101:4906–11.
9. Xiang R, Davalos AR, Hensel CH, Zhou XJ, Tse C, Naylor SL. Semaphorin 3F gene from human 3p21.3 suppresses tumor formation in nude mice. Cancer Res 2002;62:2637–43.
10. Ito I, Ji L, Tanaka F, et al. Liposomal vector mediated delivery of the 3p FUS1 gene demonstrates potent antitumor activity against human lung cancer *in vivo*. Cancer Gene Ther 2004;11:733–9.
11. Uno F, Sasaki J, Nishizaki M, et al. Myristoylation of the fus1 protein is required for tumor suppression in human lung cancer cells. Cancer Res 2004;64:2969–76.
12. Burbee DG, Forgacs E, Zochbauer-Muller S, et al. Epigenetic inactivation of RASSF1A in lung and breast cancers and malignant phenotype suppression. J Natl Cancer Inst 2001;93:691–9.
13. Divine KK, Pulling LC, Marron-Terada PG, et al. Multiplicity of abnormal promoter methylation in lung adenocarcinomas from smokers and never smokers. Int J Cancer 2004;114:400–5.
14. Wei MH, Latif F, Bader S, et al. Construction of a 600-kilobase cosmid clone contig and generation of a transcriptional map surrounding the lung cancer tumor suppressor gene (TSG) locus on human chromosome 3p21.3: progress toward the isolation of a lung cancer TSG. Cancer Res 1996;56:1487–92.
15. Timmer T, Terpstra P, van den Berg A, et al. A comparison of genomic structures and expression patterns of two closely related flanking genes in a critical lung cancer region at 3p21.3. Eur J Hum Genet 1999;7:478–86.
16. Oh JJ, West AR, Fishbein MC, Slamon DJ. A candidate tumor suppressor gene, H37, from the human lung cancer tumor suppressor locus 3p21.3. Cancer Res 2002;62:3207–13.
17. Scanlan MJ, Gordan JD, Williamson B, et al. Antigens recognized by autologous antibody in patients with renal-cell carcinoma. Int J Cancer 1999;83:456–64.
18. Welling DB, Lasak JM, Akhmametyeva E, Ghaheri B, Chang LS. cDNA microarray analysis of vestibular schwannomas. Otol Neurotol 2002;23:736–48.
19. Edamatsu H, Kaziro Y, Itoh H. LUCA15, a putative tumour suppressor gene encoding an RNA-binding nuclear protein, is down-regulated in ras-transformed Rat-1 cells. Genes Cells 2000;5:849–58.
20. Mourtada-Maarabouni M, Sutherland LC, Williams GT. Candidate tumour suppressor LUCA-15 can regulate multiple apoptotic pathways. Apoptosis 2002;7:421–32.
21. Sutherland LC, Lerman M, Williams GT, Miller BA. LUCA-15 suppresses CD95-mediated apoptosis in Jurkat T cells. Oncogene 2001;20:2713–9.
22. Rintala-Maki ND, Sutherland LC. LUCA-15/RBM5, a putative tumour suppressor, enhances multiple receptor-initiated death signals. Apoptosis 2004;9:475–84.
23. Sutherland LC, Edwards SE, Cable HC, et al. LUCA-15-encoded sequence variants regulate CD95-mediated apoptosis. Oncogene 2000;19:3774–81.
24. Mourtada-Maarabouni M, Sutherland LC, Meredith JM, Williams GT. Simultaneous acceleration of the cell cycle and suppression of apoptosis by splice variant delta-6 of the candidate tumour suppressor LUCA-15/RBM5. Genes Cells 2003;8:109–19.
25. Ramaswamy S, Ross KN, Lander ES, Golub TR. A molecular signature of metastasis in primary solid tumors. Nat Genet 2003;33:49–54.
26. Sambrook J, Fritsch EF, Maniatis T. Molecular cloning: a laboratory manual. Cold Spring Harbor (NY): Cold Spring Harbor Laboratory Press; 1989.
27. Iwasaka T, Zheng PS, Ouchida M, Yamasaki H, Yokoyama M, Sugimori H. Cytologic changes in two cervical carcinoma cell lines after transfection of the wild-type p53 gene. Acta Obstet Gynecol Scand 1996;75:797–803.
28. Sherr CJ. The Pezcoller lecture: cancer cell cycles revisited. Cancer Res 2000;60:3689–95.
29. Israels LG, Israels ED. Apoptosis. Stem Cells 1999;17:306–13.
30. Rincon JC, Engler SK, Hargrove BW, Kunkel GR. Molecular cloning of a cDNA encoding human SPH-binding factor, a conserved protein that binds to the enhancer-like region of the U6 small nuclear RNA gene promoter. Nucleic Acids Res 1998;26:4846–52.
31. Schaub M, Myslinski E, Schuster C, Krol A, Carbon P. Staf, a promiscuous activator for enhanced transcription by RNA polymerases II and IIII. EMBO J 1997;16:173–81.
32. Sutherland LC, Rintala-Maki ND, White RD, Morin CD. RNA binding motif (RBM) proteins: a novel family of apoptosis modulators? J Cell Biochem 2005;94:5–24.
33. Drabkin HA, West JD, Hotfilder M, et al. DEF-3(g16/NY-LU-12), an RNA binding protein from the 3p21.3 homozygous deletion region in SCLC. Oncogene 1999;18:2589–97.
34. Audic Y, Hartley RS. Post-transcriptional regulation in cancer. Biocell 2004;96:479–98.